AGU PUBLICATIONS

JGR

Journal of Geophysical Research: Atmospheres

RESEARCH ARTICLE
10.1002/2016JD024952

Key Points:
- Agreement between model and TES PAN measurements
- Anthropogenic and soil NOx are the major sources of Asian free tropospheric PAN
- Important contribution (about 30%) of PAN on transpacific O3 transport

Correspondence to:
Z. Jiang,
zhejiang@ucar.edu

Citation:
Jiang, Z., J. R. Worden, V. H. Payne, L. Zhu, E. Fischer, T. Walker, and D. B. A. Jones (2016), Ozone export from East Asia: The role of PAN, *J. Geophys. Res. Atmos., 121*, 6555–6563, doi:10.1002/2016JD024952.

Received 16 FEB 2016
Accepted 18 MAY 2016
Accepted article online 20 MAY 2016
Published online 7 JUN 2016

Ozone export from East Asia: The role of PAN

Zhe Jiang[1,2], John R. Worden[1], Vivienne H. Payne[1], Liye Zhu[3], Emily Fischer[3], Thomas Walker[1], and Dylan B. A. Jones[4]

[1]Jet Propulsion Laboratory, California Institute of Technology, Pasadena, California, USA, [2]Now at National Center for Atmospheric Research, Boulder, Colorado, USA, [3]Department of Atmospheric Science, Colorado State University, Fort Collins, Colorado, USA, [4]Department of Physics, University of Toronto, Toronto, Ontario, Canada

Abstract Peroxyacetyl nitrate (PAN) is an important ozone (O_3) precursor. The lifetime of PAN is approximately 1 month in the free troposphere, and this allows O_3 production to occur in pollution plumes at intercontinental distances from its source. In this study we use the Goddard Earth Observing System (GEOS)-Chem global chemical transport model, new satellite measurements of PAN from the Aura Tropospheric Emission Spectrometer (TES), and data from the Arctic Research of the Composition of the Troposphere from Aircraft and Satellites (ARCTAS) field campaign over North America, to study the role of natural and anthropogenic Asian emissions on free tropospheric (900–400 hPa) PAN distributions and subsequent O_3 production. Using the ARCTAS data with GEOS-Chem, we show that while GEOS-Chem is unbiased with respect to the aircraft data, TES version 7 PAN data are biased high for regions with surface temperatures colder than 285 K. However, GEOS-Chem and TES measurements provide a consistent representation (within 15% difference) of PAN abundance over East Asia. Because of the good agreement between model and observations, we use the GEOS-Chem model to evaluate the sources of PAN precursors and the effect of free tropospheric PAN on the export of O_3 from Asia to North America. The GEOS-Chem model results show that the largest contributors to free tropospheric PAN over Asia and the northern Pacific are anthropogenic and soil NO_x emissions. Biomass burning emissions have important contributions to free tropospheric PAN over northern Pacific (25% in April), while the contribution from lightning over northern Pacific is significant in July (40%). Strong springtime transport in April results in more export of free tropospheric PAN and O_3 from East Asian emissions. This free tropospheric PAN contributes about 35% to the abundance of free tropospheric O_3 over western North America in spring and 25% in summer.

1. Introduction

Rapid expansion of economic activities in East Asia has resulted in a substantial increase of O_3 precursor emissions [*Itahashi et al.*, 2014; *Reuter et al.*, 2014] with important consequences for global O_3 concentrations [e.g., *Zhang et al.*, 2008; *Cooper et al.*, 2010; *Brown-Steiner and Hess*, 2011]. As an important but thermally unstable reservoir for NO_x, peroxyacetyl nitrate (PAN) plays a role in the long-range transport of O_3 because it enables efficient O_3 formation far downwind from pollution sources [*Singh and Hanst*, 1981; *Fischer et al.*, 2010; *Arnold et al.*, 2015]. However, there are still large uncertainties in the distribution of free tropospheric PAN because existing measurements from aircraft and surface observations are insufficient to fully test global chemistry and transport models. Key model uncertainties include our knowledge of the emissions of nonmethane volatile organic compounds, their oxidation chemistry, and poorly characterized fire injection heights [e.g., *Fischer et al.*, 2014].

Using a recently modified Goddard Earth Observing System (GEOS)-Chem model with an updated PAN scheme based on a collection of ground and aircraft data [*Fischer et al.*, 2014], we study the distribution and sources of Asian PAN and their influences on subsequent O_3 production. Measurements of free tropospheric PAN from the Aura Tropospheric Emission Spectrometer (TES) satellite instrument provide new opportunities to evaluate this model simulation due to improved spatial and temporal coverage compared with existing in situ measurements [*Payne et al.*, 2014]. In recent work, this new data set has been applied to investigate the interannual variation of free tropospheric PAN and its relationship to biomass burning and convection in boreal Asia [*Zhu et al.*, 2015].

The transpacific transport of East Asia pollution varies seasonally. For example, transpacific transport tends to be faster in spring because of stronger westerly winds [e.g., *Liang et al.*, 2005]. In addition, *Jiang et al.* [2015] found that the O_3 production efficiency over East Asia is approximately 2 times higher in summer than in spring. In this research, we will investigate the seasonal variations of East Asian O_3 and PAN and the contribution

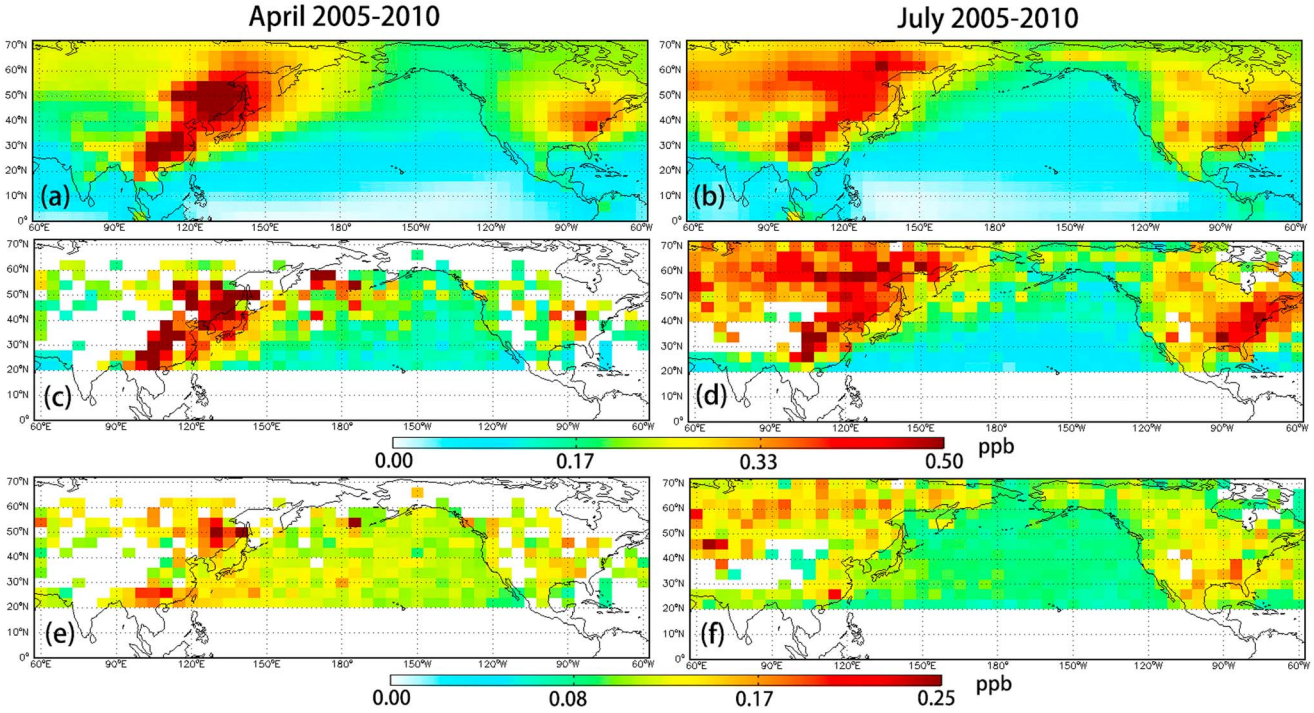

Figure 1. Multiyear monthly mean estimates of free tropospheric PAN (900–400 hPa) in April and July 2005–2010. (a and b) GEOS-Chem simulation; (c and d) GEOS-Chem simulation, sampled at TES measurement locations and times; and (e and f) GEOS-Chem simulation, smoothed with TES PAN averaging kernels. The white spaces indicate regions with no data. Please note the different color scales among panels.

of East Asian PAN to transpacific O_3 transport during spring and summer, particularly the variation associated with the varying dynamics and O_3 production efficiency.

This paper is organized as follows: in section 2 we describe the GEOS-Chem model and the TES PAN retrievals used in this work along with an evaluation of the model using measurements from TES and the Arctic Research of the Composition of the Troposphere from Aircraft and Satellites (ARCTAS) field campaign. In section 3 we examine the sources of East Asian PAN using a sensitivity analysis approach. We discuss the role of East Asian PAN in the transpacific transport of O_3 in section 4. Our conclusions follow in section 5.

2. Asian PAN Distribution From Model and Observations

We use the GEOS-Chem chemical transport model (http://www.geos-chem.org) to simulate PAN and its contribution to O_3 production at $4° \times 5°$ horizontal resolution. The model (v9-01-01) is driven by assimilated meteorological observation from the NASA Goddard Earth Observing System (GEOS-5) at the Global Modeling and data Assimilation Office (GMAO). We use the updated PAN scheme described in *Fischer et al.* [2014]. Figures 1a and 1b show the simulated multiyear monthly mean free tropospheric PAN (900–400 hPa) in April and July, for the years 2005–2010. The model shows high PAN volume mixing ratios (VMRs) over East Asia and the Eastern U.S., associated with strong anthropogenic NO_x emissions, and high PAN VMRs over boreal Asia, associated with both anthropogenic and biomass burning emissions [*Zhu et al.*, 2015].

The Aura TES satellite instrument [*Beer et al.*, 2001], flying since 2004, measures thermal infrared radiances in the nadir view at high spectral resolution (0.1 cm^{-1} apodized). These radiances contain information on a number of different trace gases, including PAN. Here we use results from a prototype algorithm corresponding to the approach that is implemented to produce the TES v7 PAN product. One difference between the prototype retrievals used here and the TES v7 product is that these retrievals use a uniform "unpolluted" prior profile in all cases, while the v7 retrievals use a variable prior as described in *Payne et al.* [2014]. TES trace gas retrievals are performed using an optimal estimation approach with a priori constraints [*Rodgers*, 2000; *Bowman et al.*, 2006; *Payne et al.*, 2014]. TES can measure elevated PAN, with a detection limit of approximately 0.2 ppbv and uncertainties between 30% and 50%. The detection limit, as described in *Payne et al.* [2014], is related to the maximum

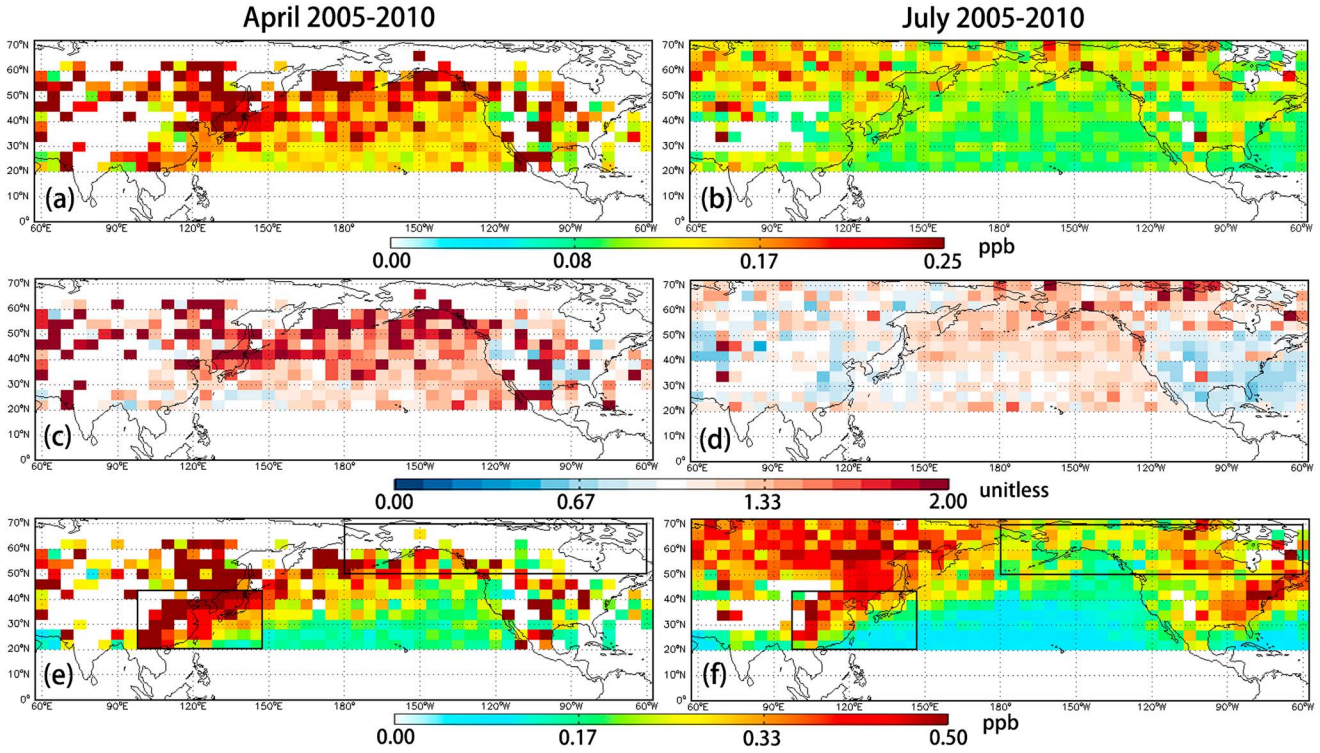

Figure 2. Multiyear monthly mean estimates of free tropospheric PAN (900–400 hPa) in April and July 2005–2010. (a and b) TES PAN measurements; (c and d) Scaling factors, defined as the ratio of TES PAN measurements over smoothed model; and (e and f) GEOS-Chem simulation, adjusted with the scaling factors. The white spaces indicate regions with no data. The black boxes define the East Asian and Boreal North America regions referred to in the text. Please note the different color scales among panels.

value of the PAN profile in the free troposphere. If the profile in the free troposphere gets above 0.2 ppb, then TES can likely observe the PAN signal in the measured radiances. The number of degrees of freedom for signal (DOFS), or independent pieces of vertical information in the TES PAN retrievals, is generally less than 1 and the sensitivity of the TES PAN retrievals peaks in the free troposphere. For this work, we have screened the TES PAN data to exclude retrievals where (1) the DOFS is less than 0.6 (indicating that the estimated PAN captures at least 60% of the true PAN variability); (2) the chi-square value is larger than 1.5, in order to remove data where the spectra were not well fit; (3) the surface temperature is lower than 275 K, in order to avoid biases associated with the impact of ice/snow emissivity on the PAN retrieval. The TES PAN retrievals used in this work were run with a globally uniform unpolluted a priori profile.

Figures 1c and 1d show the modeled free tropospheric PAN, sampled at TES PAN measurement locations and times. White spaces indicate regions with no data. Comparing a model simulation with the TES PAN observations requires accounting for the vertical resolution and a priori constraints used to infer PAN concentrations from TES radiance measurements [e.g., *Payne et al.*, 2014]. The vertical resolution is accounted for with the averaging kernel, which represents the sensitivity of the retrieval to the atmospheric distribution of the estimated trace gas. The TES optimal estimation retrieval algorithm produces an averaging kernel for each individual TES observation. Figures 1e and 1f show the modeled free tropospheric PAN, smoothed with TES averaging kernels. The spatial variations in PAN VMR decrease significantly in going from the sampled model to the smoothed model, because of the global uniform unpolluted a priori profile used in these retrievals. Nonetheless, the model results in Figures 1a and 1b, the sampled model results in Figures 1c and 1d, and the smoothed model results in Figures 1e and 1f all show a contrast between PAN over land versus ocean, particularly in July, demonstrating the sensitivity of the TES PAN retrievals to these type of spatial gradients in the free troposphere.

Figures 2a and 2b show the observed multiyear monthly mean free tropospheric PAN from TES. Due to the influence of the choice of the prior profiles on the retrieval, these fields will represent a smoothed version of the true spatial variation in PAN. On the other hand, the a priori profile has no influence on data assimilation, because the smoothing errors are completely removed when the modeled profiles are smoothed using

averaging kernels. In this work, we focused on the consistency between model and TES measurements. There are two possible methods for model and data comparison:

1. PAN_{smooth} versus PAN_{TES}
2. PAN_{model} versus $PAN_{model} \times (PAN_{TES}/PAN_{smooth}) = PAN_{adjusted}$

Here PAN_{model} is the model sampled at TES times and locations, PAN_{TES} is the TES PAN retrieval, and PAN_{smooth} is the "smoothed model," with the TES PAN averaging kernels and a priori applied to the original model simulation. The ratio of PAN_{TES}/PAN_{smooth} is used as a scaling factor and applied to PAN_{model} to create an "adjusted model" PAN distribution. For the purposes of model evaluation, these two methods will result in the same conclusion. However, in the case of the data set used in this work, the PAN VMRs in the smoothed model (Figures 1e and 1f) will be unrealistically small because of the background a priori used in this set of retrievals, while the adjusted model provides more realistic PAN VMRs. Therefore, in the analysis that follows, we choose to use the adjusted model. Figures 2c and 2d show the scaling factors, which are generally close to one, except at high latitudes in spring. Figures 2e and 2f show the model adjusted with the scaling factors.

Figures 3a and 3b show scatterplots comparing modeled free tropospheric PAN (Figures 1c and 1d) over East Asia (defined as black box shown in Figures 2e and 2f) with the adjusted model. The result demonstrates good consistency between the model and data in both seasons for warmer cases. However, for cases where the surface temperature is lower than 285 K, the adjusted model is higher (up to 40%) than the original model. The surface temperature here is a convenient variable for visualization, but it is likely that the physical reason for the bias would be associated with the atmospheric temperature rather than the surface temperature. One possible way that a temperature-dependent bias could occur in the TES PAN retrievals would be through an error in the temperature dependence of the absorption cross sections used in the forward model. This is a topic for future investigation.

In order to further investigate the temperature-dependent discrepancy between the original and the adjusted model, we evaluate our model simulation using data from the NASA ARCTAS field campaign [*Alvarado et al.*, 2010]. Figure 4 shows the coverage of ARCTAS aircraft, for the period of 1–19 April and 29 June to 13 July 2008, over boreal North America. Figures 3c and 3d show scatterplots comparing the original model and the adjusted model using TES observations for boreal North America (defined by the box in Figure 2). Again, there is an apparent temperature-dependent bias between the original and adjusted model. Figures 3e and 3f show comparisons between the model simulation and the ARCTAS aircraft measurements over Boreal North America (50°N–70°N). The model simulation shows generally good agreement with the aircraft measurements for PAN values below 0.4 ppb. There is considerable scatter in the model/aircraft comparisons, particularly at the higher PAN values, where the aircraft is sampling plumes that may not be well represented in the model. However, there is no apparent temperature dependence in the model/aircraft comparisons. These results indicate a possible temperature-dependent high bias in the TES PAN retrievals, particularly in high-latitude regions with colder temperatures, as shown in Figure 2c. It should be mentioned that this conclusion is only based on the model/data comparison in April and July. More analyses are needed in the future for a more robust evaluation of the TES data. For this reasons we focus our analysis on lower latitude regions such as East Asia where we expect this bias to be minimal.

Some caution is required in interpreting the model and data comparison because TES cannot observe the low PAN values. Figure 5 shows histogram plots comparing multiyear monthly mean estimates of free tropospheric PAN over East Asia in April/July 2005–2010 for both original model and model adjusted with TES PAN measurements. Our result shows that 80% free tropospheric PAN concentrations, from both model and adjusted model, are higher than the detection limit (0.2 ppb) in April. There are more low PAN values in July, but the majority of low PAN concentrations are over ocean (Figure 1d). Further considering (1) the long (~500 km or more) length scales of the free-troposphere mean that the observed PAN observations are correlated with nearby PAN values [e.g., *Dupont et al.*, 2012] and (2) we sample the GEOS-Chem at the same spatiotemporal locations as the TES observations, we believe that our conclusion about the good consistency between model and TES PAN retrievals over East Asia is not likely affected by this sampling bias, particularly over land.

3. Sources of Asian Free Tropospheric PAN

The agreement between model and data allows us to use the model to examine the processes and emissions controlling the distribution of free tropospheric PAN and its contribution to O_3 production as discussed

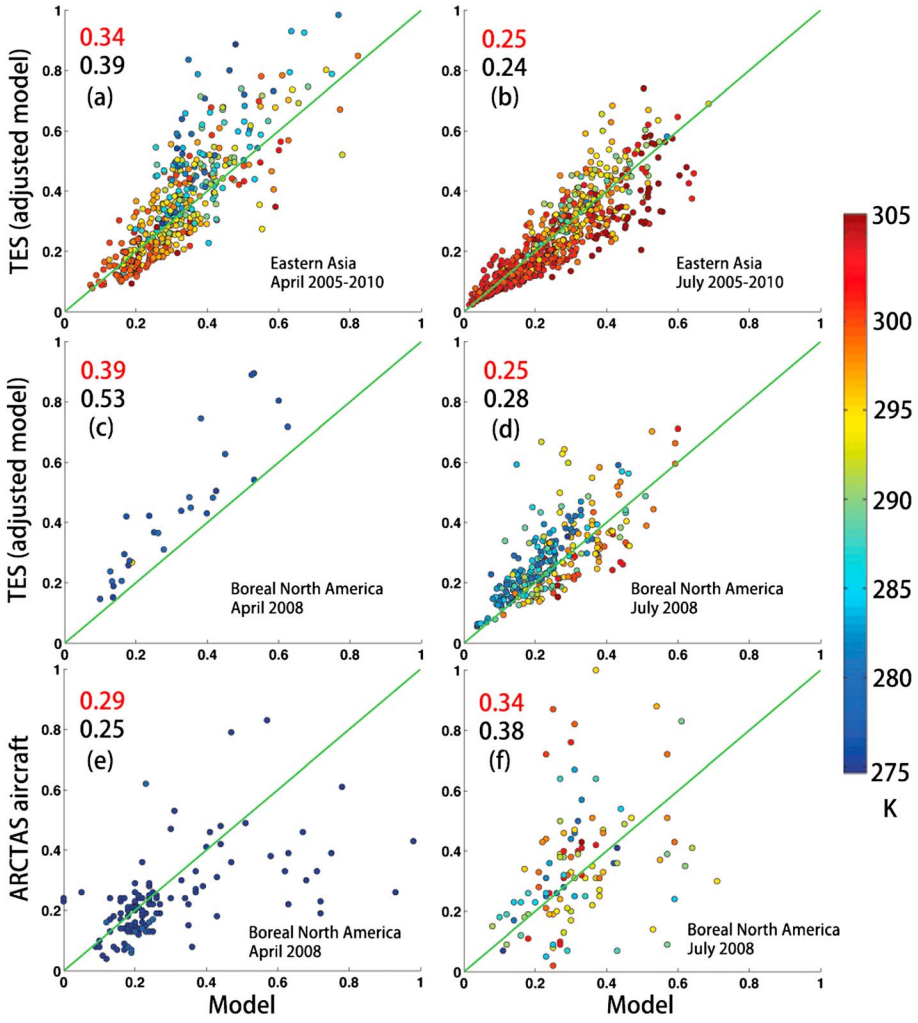

Figure 3. Scatterplots comparing modeled PAN with TES (adjusted model) and ARCTAS aircraft measurements (900–400 hPa). The unit is ppb. The color scale shows GMAO ground/sea surface temperature. (a and b) Model simulation with TES for April/July 2005–2010 over East Asia. (c and d) Model simulation with TES for April/July 2008 over Boreal North America. (e and f) Model simulation with ARCTAS aircraft measurements for April/July 2008 over Boreal North America (50°N–70°N). The model simulation was sampled at aircraft measurment locations, altitudes, and times and was averaged for grid box. The top-left numbers are the mean value of model (red) and measurements (black). The East Asia and boreal North America domains are defined in Figure 2.

below. In order to evaluate the sources of Asian PAN, we turnoff East Asian NO_x emissions (anthropogenic, soil, and biomass burning) in the GEOS-Chem model for the periods March–May and June–August 2005–2010 to investigate their influences on the PAN distribution. Figure 6 shows the model results in April and July 2005–2010. As shown in Figures 6a and 6b, East Asian NO_x emissions support significant PAN formation over East China, and the magnitude of East China PAN is higher in April. The simulated East Asian PAN export over the Pacific ocean is higher in April, reflecting the contributions of larger PAN formation from China and stronger westerly winds [e.g., *Liang et al.*, 2005].

Figures 6c and 6d show the background PAN, produced from anthropogenic (fossil fuels and biofuels) and soil NO_x emissions outside of East Asia; Figures 6e and 6f show the background PAN, produced from biomass burning NO_x emissions, outside of East Asia; Figures 6g and 6h show the PAN produced from lightning NO_x. These results indicate that anthropogenic and soil NO_x emissions, from both East Asia and Rest of World, are the largest contributions to free tropsopheric PAN over Asia and Northern Pacific Ocean. The contribution from biomass burning emissions is smaller than anthropogenic and soil emissions over East Asia, but is an important source over northern Pacific (25% in April), while the contribution from lightning over northern

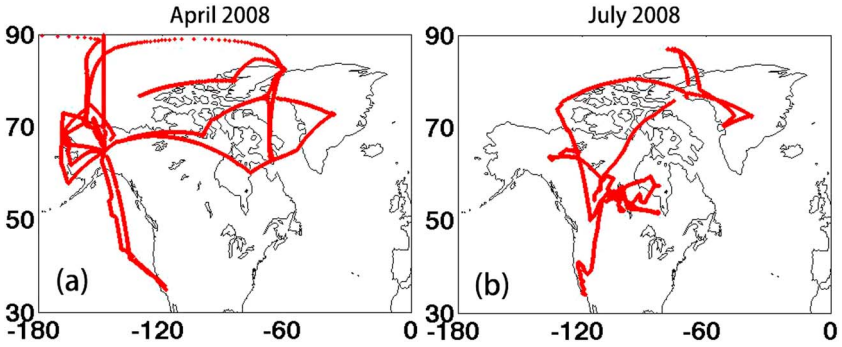

Figure 4. Trajectories of ARCTAS aircraft in 1–19 April and 29 June to 13 July 2008. Free tropospheric PAN measurements (900–400 hPa) between 50°N and 70°N are used in this work.

Pacific is significant in July (40%). However, it is quite possible that a different distribution of PAN precursors could result in a similar PAN distribution as represented by the model. Consequently, additional studies are needed to quantify the partitioning of the different PAN precursor sources; these studies can be conducted with a larger set of TES data because the spatial distributions of free tropospheric PAN could be used to identify and quantify surface PAN precursor emissions.

4. Role of East Asian PAN on Long-Range O_3 Transport

The seasonality of PAN mixing ratios resulting from Asian emissions is an important driver of how much O_3 is exported from Asia either (1) directly after formation from surface emissions or (2) through downwind production as a result of the thermal decomposition of PAN back to NO_2. In a previous work, *Walker et al.* [2010] estimated the contribution of anthropogenic PAN to long-range O_3 transport by turning off PAN formation in the GEOS-Chem model. However, this approach can overestimate O_3 production over East Asia and underestimate the PAN contribution to ozone because PAN serves as a major NO_x sink in East Asia and removing that sink enhances O_3 production. We address this issue by running GEOS-Chem using the following steps:

1. Run the GEOS-Chem model without East Asian NO_x
2. Store background PAN distributions
3. Run the GEOS-Chem model with East Asian NO_x emissions
4. At each time step we re-write the free-tropospheric PAN fields over a region (97.5–180°E, 20–60°N) significantly affected by East Asian emissions (Figures 6a and 6b) in reference model with background PAN concentrations from Step 2.

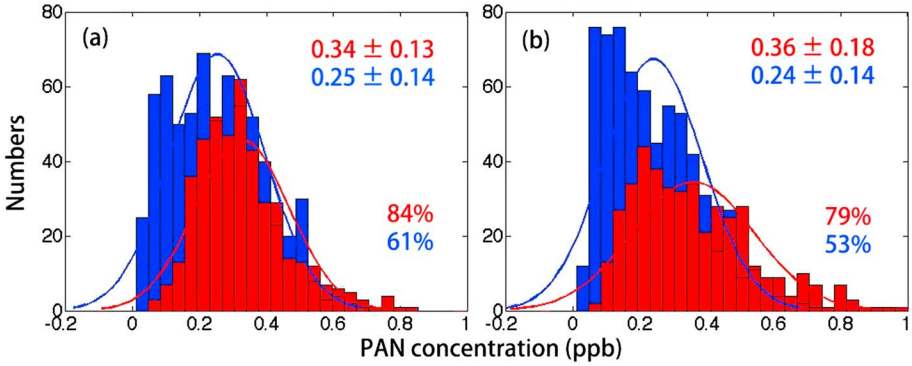

Figure 5. Histogram plots comparing multkiyear monthly mean estimates of free tropospheric PAN (900–400 hPa) over East Asia in April (red) and July (blue) 2005–2010. (a) GEOS-Chem simulation, sampled at TES measurment locations and times; (b) GEOS-Chem simulation, adjusted with TES PAN measurements. The numbers are mean value ± standard deviation, and percents of concentrations larger than the detection limit (0.2 ppb).

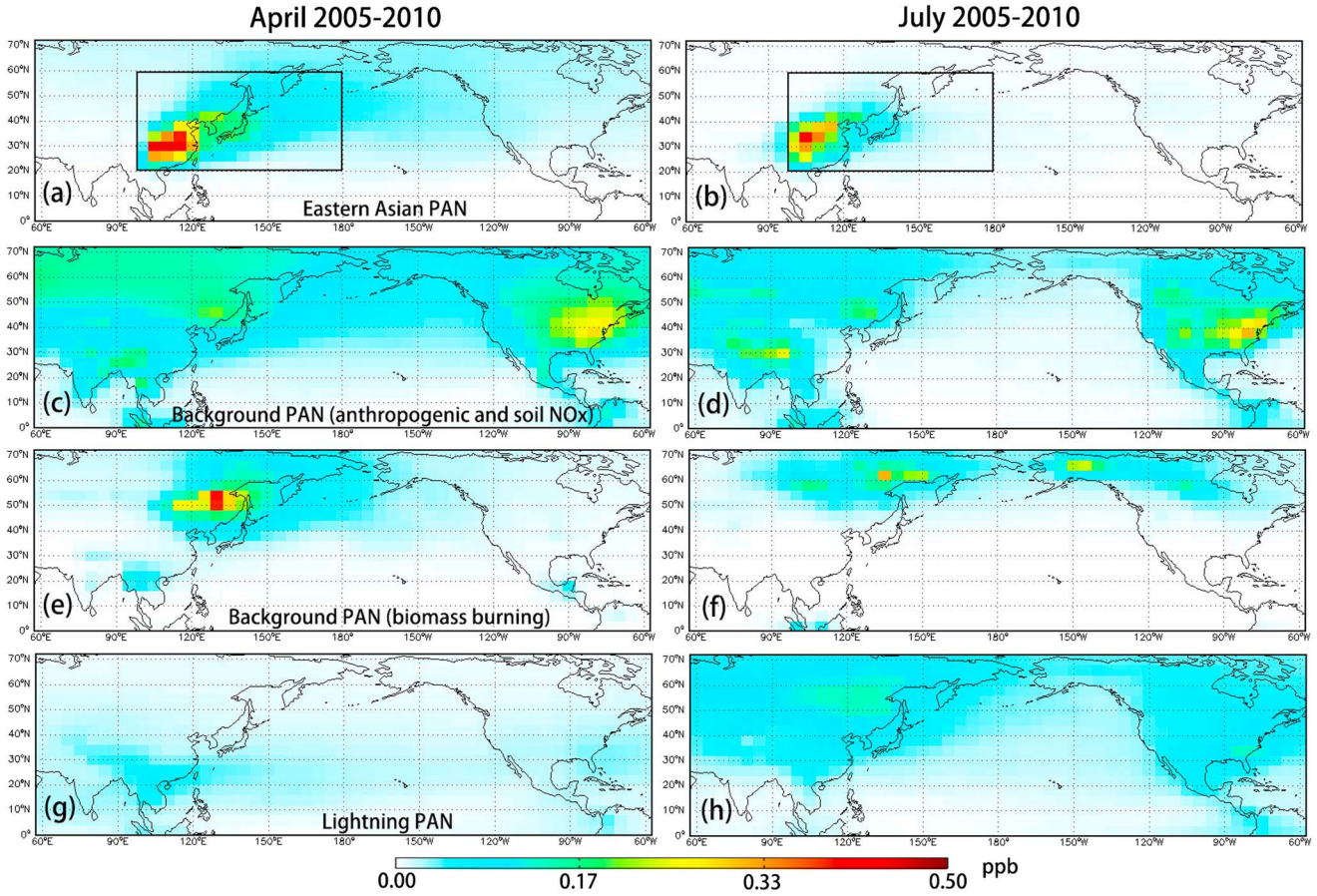

Figure 6. Multiyear monthly mean estimates of free tropospheric PAN (900–400 hPa) in April and July 2005–2010. (a and b) East Asian PAN, produced from East Asian NO_x emissions. (c and d) Background PAN, produced from anthropogenic (fossil fuels and biofuels) and soil NO_x emissions outside of East Asia. (e and f) Background PAN, produced from biomass burning NO_x emissions outside of East Asia. (g and h) PAN produced from lightning NO_x. The East Asian domain is defined in Figure 2. The black box defines the region, where background PAN is rewritten is section 4.

As shown in Figures 7a and 7b, the lower PAN field, without the East Asian contribution, reduces mean O_3 concentrations over East Asia by 2.9 ppb in summer and 1.7 ppb in spring.

The larger influence of PAN on O_3 over East Asia in the summer is due to increased production of O_3 from NO_x in the summer [e.g., *Jiang et al.*, 2015]. In contrast, the influence of free tropospheric PAN on free tropospheric O_3 concentrations over the central and East Pacific is larger in spring than that in summer due to more PAN export (Figures 6a and 6b). Figures 7c and 7d show the change of O_3 mixing ratios when East Asian NO_x emissions are removed from the simulation. The spatial features of Figures 7c and 7d are similar to those in Figures 7a and 7b but they have a larger magnitude. Over East Asia, the change in mean O_3 mixing ratios is 18.7 ppb in summer and 11.7 ppb in spring.

The ratio of the O_3 change due to free tropospheric PAN from East Asian emissions (Figures 7a and 7b) to the O_3 change due to NO_x (Figures 7c and 7d) represents the relative contribution of free tropospheric PAN to long-range O_3 transport. As shown in Figures 7e and 7f, the relative contribution of PAN is lower over Eastern China, because of strong direct O_3 production, and is higher over the ocean because PAN is a source for NO_x over the ocean where O_3 production is NO_x limited. The contribution from free tropospheric PAN to O_3 over North America is also higher in the spring (~35%) versus the summer (~25%).

For the period of 2005–2010, the contribution from East Asian emissions to western North American (122.5–97.5°W, 28–52°N) free tropospheric O_3 is only slightly higher in spring (2.9 ppb) than in summer (2.1 ppb). However, it is about 2 times higher (1.9 ppb versus 0.9 ppb) in the lower troposphere (below 900 hPa, approximately), which means that springtime export of Asian pollution has a larger effect than summertime export on surface

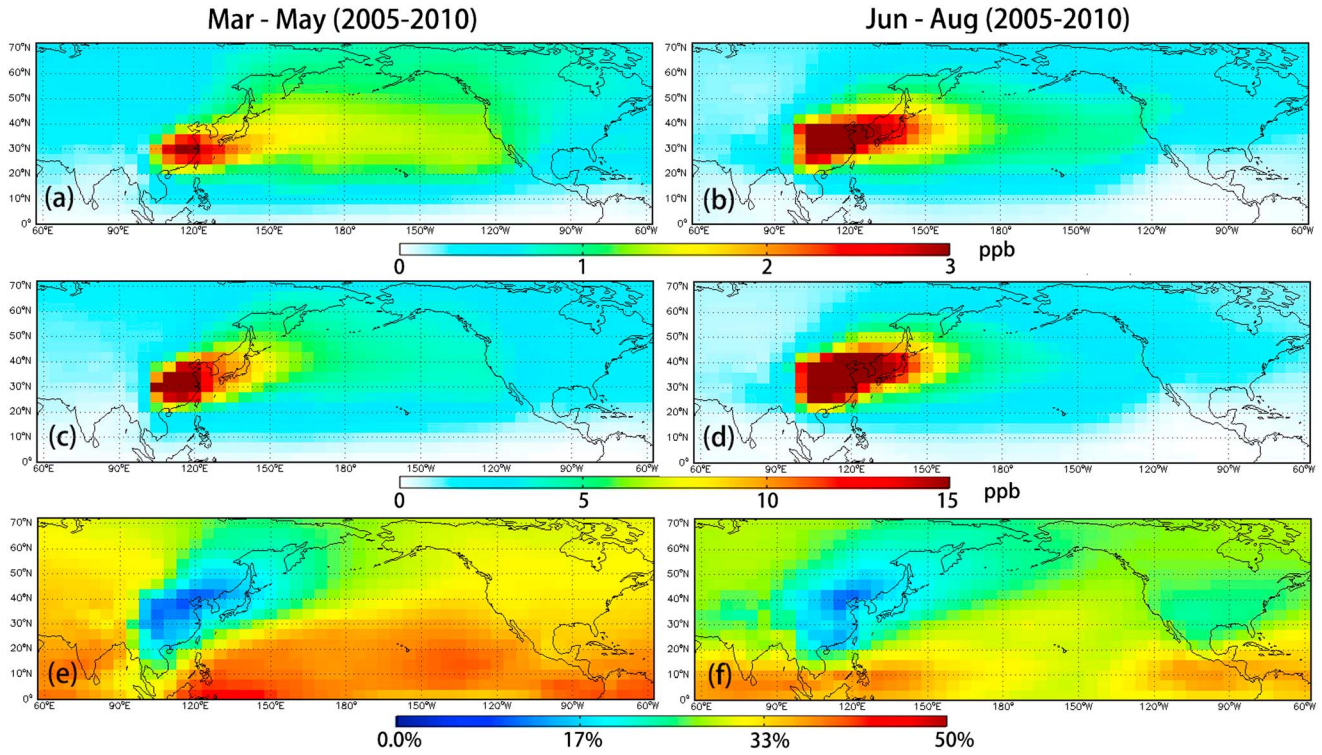

Figure 7. Multiyear seasonal mean response of free trospheric O_3 (900–400 hPa) to East Asian NO_x emissions. (a and b) O_3 produced from East Asian PAN. (c and d) O_3 produced from East Asian NO_x emission. (e and f): Relative contribution of PAN on free tropospheric O_3, calculated by Figures 7a and 7b/ Figures 7c and 7d). Please note the different color scales between Figures 7a and 7b with Figures 7c and 7d.

ozone in North America. It should be noted that our estimate (1.9 ppb) is significantly lower than the value (5–7 ppb) in *Zhang et al.* [2008] because their a priori NO_x emissions are larger by a factor of 2 than that used in our study, and because they considered the entire Asia domain (80–150°E, 8–50°N) in their study.

Previous studies [e.g., *Alvarado et al.*, 2010; *Dupont et al.*, 2012; *Arnold et al.*, 2015] have demonstrated that boreal Asian biomass burning are important sources of free tropospheric PAN. Because of the possible bias in TES PAN retrievals in higher-latitude region, we focus on the influence of East Asian emissions in this work. However, it is highly possible that biomass burning PAN will play a more critical role in free tropospheric O_3, because of the high conversion ratio from biomass burning NO_x to PAN (~40% [*Alvarado et al.*, 2010]). Consequently, more studies are needed in future to better constrain the emission magnitude, interannual variation of biomass burning PAN from boreal Asia, and their influences on global O_3 level.

5. Conclusions

We use the GEOS-Chem model with an updated PAN scheme based on ground and aircraft data [*Fischer et al.*, 2014] to study the role of natural and anthropogenic emissions on global PAN distributions and subsequent O_3 production. The model simulation is evaluated with ARCTAS field campaign PAN measurements in April/July 2008 and Aura TES PAN measurements in April/July 2005–2010. There is likely a temperature-dependent overestimation in TES PAN retrievals at high latitudes where the temperature is colder. Note that we do not expect this bias to strongly affect the conclusions of *Zhu et al.* [2015], who used TES springtime PAN data at high latitudes to quantify the role of fires on PAN, because they looked at relative differences in the TES PAN data. We conclude that for spring and summer, at lower latitudes, we can infer good consistency between model, TES, and aircraft, providing confidence in the model simulations.

Using the GEOS-Chem model, we assess the distribution and sources of Asian free tropospheric PAN, and the relative contribution of free tropospheric PAN, formed from East Asian emissions to long-range O_3 transport. Our model analysis demonstrate that anthropogenic and soil NO_x emissions have significant contributions to free tropsopheric PAN over Asia and Northern Pacific Ocean. The contribution from biomass burning

emissions is smaller, and the contribution from lightning is important in July. The relative contribution of this East Asian PAN to long-range O_3 transport is about 35% in spring and about 25% in summer. This seasonality is mainly driven by more East Asia PAN export in spring and by more direct O_3 production from NO_x over East Asia in the summer. This analysis confirms the important effects of the seasonality of PAN on the seasonality of global tropospheric O_3 abundances.

Acknowledgments
This work was supported by the NASA Award NNX14AF14G. Part of this research was carried out at the Jet Propulsion Laboratory, California Institute of Technology, under a contract with the National Aeronautics and Space Administration. The data of ARCTAS aircraft measurements were downloaded from ftp://ftp-air.larc.nasa.gov/pub/ARCTAS/MERGES/DC8/1_MINUTE/. We thank ARCTAS science team for providing their aircraft PAN measurements. The data of TES PAN measurements were provided by Vivienne H. Payne (Vivienne.H.Payne@jpl.nasa.gov).

References

Alvarado, M. J., et al. (2010), Nitrogen oxides and PAN in plumes from boreal fires during ARCTAS-B and their impact on ozone: An integrated analysis of aircraft and satellite observations, *Atmos. Chem. Phys.*, *10*, 9739–9760, doi:10.5194/acp-10-9739-2010.

Arnold, S., et al. (2015), Biomass burning influence on high latitude tropospheric ozone and reactive nitrogen in summer 2008: A multi-model analysis based on POLMIP simulations, *Atmos. Chem. Phys.*, *15*, 6047–6068, doi:10.5194/acp-15-6047-2015.

Beer, R., T. A. Glavich, and D. M. Rider (2001), Tropospheric emission spectrometer for the Earth Observing System's Aura satellite, *Appl. Opt.*, *40*, 2356–2367.

Bowman, K. W., et al. (2006), Tropospheric emission spectrometer: Retrieval method and error analysis, *IEEE Trans. Geosci. Remote Sens.*, *44*(5), 1297–1307, doi:10.1109/TGRS.2006.871234.

Brown-Steiner, B., and P. Hess (2011), Asian influence on surface ozone in the United States: A comparison of chemistry, seasonality, and transport mechanisms, *J. Geophys. Res.*, *116*, D17309, doi:10.1029/2011JD015846.

Cooper, O. R., et al. (2010), Increasing springtime ozone mixing ratios in the free troposphere over western North America, *Nature*, *463*, 344–348, doi:10.1038/nature08708.

Dupont, R., et al. (2012), Attribution and evolution of ozone from Asian wild fires using satellite and aircraft measurements during the ARCTAS campaign, *Atmos. Chem. Phys.*, *12*, 169–188.

Fischer, E. V., D. A. Jaffe, D. R. Reidmiller, and L. Jaeglé (2010), Meteorological controls on observed peroxyacetyl nitrate at Mount Bachelor during the spring of 2008, *J. Geophys. Res.*, *115*, D03302, doi:10.1029/2009JD012776.

Fischer, E. V., et al. (2014), Atmospheric peroxyacetyl nitrate (PAN): A global budget and source attribution, *Atmos. Chem. Phys.*, *14*(5), 2679–2698, doi:10.5194/acp-14-2679-2014.

Itahashi, S., I. Uno, H. Irie, J.-I. Kurokawa, and T. Ohara (2014), Regional modeling of tropospheric NO_2 vertical column density over East Asia during the period 2000–2010: Comparison with multisatellite observations, *Atmos. Chem. Phys.*, *14*(7), 3623–3635, doi:10.5194/acp-14-3623-2014.

Jiang, Z., J. R. Worden, D. B. A. Jones, J.-T. Lin, W. W. Verstraeten, and D. K. Henze (2015), Constraints on Asian ozone using Aura TES, OMI and Terra MOPITT, *Atmos. Chem. Phys.*, *15*, 99–112, doi:10.5194/acp-15-99-2015.

Liang, Q., L. Jaeglé, and J. Wallace (2005), Meteorological indices for Asian outflow and transpacific transport on daily to interannual timescales, *J. Geophys. Res.*, *110*, D18308, doi:10.1029/2005JD005788.

Payne, V., M. Alvarado, K. Cady-Pereira, J. Worden, S. Kulawik, and E. Fischer (2014), Satellite observations of peroxyacetyl nitrate from the Aura Tropospheric Emission Spectrometer, *Atmos. Meas. Tech.*, *7*(11), 3737–3749, doi:10.5194/amt-7-3737-2014.

Reuter, M., M. Buchwitz, A. Hilboll, A. Richter, O. Schneising, M. Hilker, J. Heymann, H. Bovensmann, and J. Burrows (2014), Decreasing emissions of NO_x relative to CO_2 in East Asia inferred from satellite observations, *Nat. Geosci.*, *7*(11), 792–795, doi:10.1038/ngeo2257.

Rodgers, C. D. (2000), *Inverse Methods for Atmospheric Sounding: Theory and Practice*, World Sci., Hackensack, N. J.

Singh, H. B., and P. L. Hanst (1981), Peroxyacetyl nitrate (PAN) in the unpolluted atmosphere: An important reservoir for nitrogen oxides, *Geophys. Res. Lett.*, *8*, 941–944, doi:10.1029/GL008i008p00941.

Walker, T., et al. (2010), Trans-Pacific transport of reactive nitrogen and ozone to Canada during spring, *Atmos. Chem. Phys.*, *10*(17), 8353–8372, doi:10.5194/acp-10-8353-2010.

Zhang, L., et al. (2008), Transpacific transport of ozone pollution and the effect of recent Asian emission increases on air quality in North America: An integrated analysis using satellite, aircraft, ozonesonde, and surface observations, *Atmos. Chem. Phys.*, *8*(20), 6117–6136, doi:10.5194/acp-8-6117-2008.

Zhu, L., E. V. Fischer, V. H. Payne, J. R. Worden, and Z. Jiang (2015), TES observations of the interannual variability of PAN over Northern Eurasia and the relationship to springtime fires, *Geophys. Res. Lett.*, *42*, 7230–7237, doi:10.1002/2015GL065328.